

ORIGINS OF COMPLEX SEISMIC ANISOTROPY BENEATH THE WALLOWA  
MOUNTAINS, NORTHEAST OREGON

by

WILLIAM BARTHOLOMEW NIDAY

A THESIS

Presented to the Department of Earth Sciences  
and the Graduate School of the University of Oregon  
in partial fulfillment of the requirements  
for the degree of  
Master of Science

September 2019

THESIS APPROVAL PAGE

Student: William Bartholomew Niday

Title: Origins of Complex Seismic Anisotropy beneath the Wallowa Mountains,  
Northeast Oregon

This thesis has been accepted and approved in partial fulfillment of the  
requirements for the Master of Science degree in the Department of Earth  
Sciences by:

Gene Humphreys	Chairperson
Diego Melgar	Member
Valerie Sahakian	Member

and

Janet Woodruff-Borden Vice Provost and Dean of the Graduate School

Original approval signatures are on file with the University of Oregon Graduate  
School.

Degree awarded September 2019

© 2019 William Bartholomew Niday

This work is licensed under a Creative Commons  
**Attribution-NonCommercial-NoDerivs 4.0**  
International License.



## THESIS ABSTRACT

William Bartholomew Niday

Master of Science

Department of Earth Sciences

September 2019

Title: Origins of Complex Seismic Anisotropy beneath the Wallowa Mountains,  
Northeast Oregon

We use a dense network of observations and an automated method of analysis to investigate complex patterns of seismic anisotropy in eastern Oregon. We present SKS splitting results for approximately 220 broadband seismic stations in the Pacific Northwest, including 33 stations from the new Wallowa2 array deployed between 2016 and 2018 in northeast Oregon. Our data set contains approximately 3300 splitting measurements.

Over most of the Pacific Northwest, SKS splitting is consistent with a conceptual model of broadly east-west mantle flow redirected in places by lithospheric strength variations. However, splitting analysis performs poorly in northeast Oregon, and results are not consistent with uniform or layered anisotropy. We argue that anisotropy in NE Oregon is laterally heterogeneous on small scale, and propose a model that attributes complex splitting behavior to the seismically imaged Wallowa high-velocity anomaly.

## ACKNOWLEDGMENTS

The facilities of IRIS Data Services, and specifically the IRIS Data Management Center, were used for access to waveforms, related metadata, and/or derived products used in this study. IRIS Data Services are funded through the Seismological Facilities for the Advancement of Geoscience and EarthScope (SAGE) Proposal of the National Science Foundation under Cooperative Agreement EAR-1261681.

## CURRICULUM VITAE

NAME OF AUTHOR: William Bartholomew Niday

### GRADUATE AND UNDERGRADUATE SCHOOLS ATTENDED:

University of Oregon, Eugene  
University of Nevada, Reno

### DEGREES AWARDED:

Master of Science, Earth Sciences, 2019, University of Oregon  
Bachelor of Science, Geological Engineering, 2015, University of Nevada,  
Reno

### AREAS OF SPECIAL INTEREST:

Seismology  
Geodynamics  
Geomechanics

### PROFESSIONAL EXPERIENCE:

Graduate Employee, University of Oregon, 2016-2019

### PUBLICATIONS:

Castellanos, J. C., Perry-Houts, J., Clayton, R. W., Kim, Y., Stanciu, A. C., Niday, B., & Humphreys, E. (2019b). Seismic anisotropy reveals crustal flow driven by mantle vertical loading in the Pacific NW. Under review in *Nature Geoscience*.

## TABLE OF CONTENTS

Chapter	Page
I. INTRODUCTION .....	1
Previous Work.....	4
II. METHODS .....	5
Data Collection .....	5
Splitting Measurement.....	6
III. RESULTS AND DISCUSSION .....	9
SKS Splits .....	9
Complex Anisotropy.....	11
Finite Frequency Modeling.....	13
IV. CONCLUSIONS .....	16
APPENDIX: FIGURES .....	18
REFERENCES CITED .....	27

## LIST OF FIGURES

Figure	Page
1. Location of the broadband seismic stations .....	18
2. Distribution of earthquakes and number of seismograms.....	19
3. Non-null splitting results plotted at piercing points .....	20
4. Splitting estimates for stations .....	21
5. Average one-layer splitting estimates.....	22
6. Synthetic example of cross-convolution .....	23
7. Cross-convolution misfit $E(m)$ .....	24
8. Two-layer anisotropic models.....	25
9. Finite-frequency synthetic model .....	26



## I: INTRODUCTION

Because shear deformation in the upper mantle produces a lattice preferred orientation (LPO) of anisotropic mineral crystals (mostly olivine), observations of seismic anisotropy can provide a valuable constraint on the geometry of mantle flow. Measuring the splitting of core-refracted shear waves such as SKS is one of the most well-studied and direct ways of quantifying seismic anisotropy. Because of its near vertical incidence, SKS splitting provides good constraints on lateral variation of anisotropy but little direct information about vertical variation. Furthermore, standard methods for shear-wave splitting analysis make important assumptions about the nature of anisotropy (that the seismic wave only samples one anisotropic system, which lies in the horizontal plane) and of the seismic waves (that seismic waves are only sensitive to material along the raypath). If these assumptions do not hold, such as if the upper mantle is strongly heterogeneous on the scale of seismic wavelengths, the relationship between shear-wave splitting and anisotropy may be complex.

The upper mantle in the Pacific Northwest is strongly heterogeneous on the scale of seismic wavelengths. Prominent seismically imaged structures in the Pacific Northwest are the high-velocity Juan de Fuca slab, low-velocity anomalies under north central Oregon and the Snake River Plain, and two separate high-velocity bodies beneath northeast Oregon and northern Idaho. Darold and Humphreys (2013) argue that the latter structures are fragments of Farallon oceanic lithosphere that detached from the North American continent at

approximately 16 and 53 Ma, respectively. Mantle flow associated with their detachment would have occurred from 55-16 Ma; however, for the overall pattern of mantle flow other factors, such as Cascadia slab rollback (e.g., Druken et al., 2011) and plume flattening (e.g., Lowry et al., 2000) are also likely to be important.

Geodynamic modeling studies (e.g. Becker et al., 2006; Liu and Stegman, 2011; Zhou et al., 2018; Wang and Becker, 2019) have had success matching splitting-derived anisotropy in the western US with coupled models of mantle flow and fabric development. In general, geodynamic models agree that east-west oriented anisotropy in the PNW is due to east-directed mantle flow (relative to the North American plate). However, geodynamic models do not perform well at matching smaller-scale variations in anisotropy. Wang and Becker (2019) find that including strong cratonic roots and continental-scale mantle density structure inferred from seismic images significantly improves predicted anisotropy over models of plate-driven flow alone, but including higher-resolution models of density and craton geometry does not improve the fit to observations. Because the regional models perform well, we believe the assumption that anisotropy indicates horizontal mantle flow is valid, but it may not hold on small scales.

Geodetic observations indicate that crustal deformation in the Pacific Northwest is primarily as a rigid block rotation around a pole in central Idaho, with minimal strain accumulation south of the Seattle-Yakima thrust belt. The

discrepancy between crustal and mantle deformation implies either that the crust and mantle are mechanically decoupled or that the crust is strong enough to resist the basal tractions resulting from mantle flow (McCaffrey et al., 2013). Castellanos et al. (2019a, b) find that crustal anisotropy in the region (and inferred lower crustal flow) does not correlate with mantle strain, and propose a model where the crust is decoupled from lateral basal tractions. In their model the vertical loading associated with the Wallowa and Farallon high-velocity bodies drives crustal flow. Any anisotropy produced by asthenospheric flow during their detachment would likely have been overprinted by the last 16 million years of strain.

#### Previous Work

Although no studies have focused on complex anisotropy in northeast Oregon, there are several avenues of evidence in the region. Long et al. (2009) studied shear-wave splitting in eastern Oregon with the High Lava Plains and Wallowa<sup>1</sup> broadband seismic networks, finding a relatively coherent east-west fast axis orientation with very large delay times in southeast Oregon. For stations in NE Oregon, they found fewer and less consistent splitting measurements, which they attributed to a component of lithospheric anisotropy (as opposed to pure asthenospheric flow in SE Oregon).

Lin et al. (2010) fit observed shear-wave splitting with a model including surface wave measurements of crustal and uppermost mantle anisotropy and a

smoothly varying asthenosphere, which performs well in most of the western US but poorly in NE Oregon (although few measurements are available). We also note that in the shear-wave splitting database of Yang et al. (2016), there are relatively few non-null measurements for stations in northeast Oregon despite a good station and back azimuth distribution. However, the splitting times for non-null measurements in northeast Oregon are significant ( $\sim 1.2$  s), implying that the frequent null measurements are not simply a result of small or vertically oriented anisotropy.

We integrate data from the EarthScope USArray and several regional seismic arrays to investigate shear-wave splitting in the Pacific Northwest, with a focus on northeast Oregon. We use a very dense network of broadband seismic observations to characterize splitting in the tectonically complicated region of northeast Oregon, and attempt to place the complex anisotropy there in the context of regional tectonic models; in particular, to understand the role of the high-velocity Wallowa anomaly.

## II: METHODS

### Data Collection

We use data from approximately 220 broadband seismic stations in the IRIS DMC (Figure 1). These include stations from the U.S. National Seismic Network, USArray Transportable Array, Pacific Northwest Seismic Network, and several campaign seismic arrays including recently acquired data from the IDOR and Wallowa2 arrays. We obtain seismograms for earthquakes magnitude ( $m_b$  and  $m_w$ ) greater than 5.5 (usually greater than 6) and in the distance range of 85-120°, where the SKS phase amplitudes are significant. The resulting set of earthquakes is dominated by events with back azimuths between 225° and 315° (Figure 2).

Radial SKS arrivals are automatically picked using a 30 second window centered around the estimated travel time from the TauP package (Crotwell et al., 1999). An automatic quality control step discards seismograms with a signal-to-noise ratio of less than three when band-pass filtered to between 0.02 and 0.25 Hz. The automatic picks are then manually checked to remove duplicate events and instrument errors, and ensure that the SKS window does not overlap with other phases. Approximately 5000 seismograms remain after quality control.

## Splitting Measurement

The most widely used methods for measuring shear-wave splitting from an individual record are the rotation correlation method [RC] (Bowman & Ando, 1987) and transverse component minimization method [SC] (Silver & Chan, 1991), both of which are implemented in the commonly used SplitLab package (Wüstefeld et al., 2008). Both methods assume that anisotropy produces two identically shaped, orthogonally polarized pulses, implying a vertically incident ray and a single horizontal anisotropic layer. More complex anisotropy results in frequent ‘null splits’ and azimuthal variation in ‘apparent’ splitting parameters. Variations in apparent splitting at a single station can be used to identify multilayered or dipping anisotropy (e.g., Silver and Savage, 1994), but this requires better azimuthal coverage than is typically available.

This study uses the cross-convolution method [ML] of Menke and Levin (2003) to measure shear-wave splitting. ML assumes that the observed radial ( $V(t)$ ) and transverse ( $H(t)$ ) waveforms are each the convolution of a common source wavelet  $s(t)$  with the impulse response functions  $v_{true}(t)$  and  $h_{true}(t)$ . If an anisotropic model  $m$  has impulse responses  $v(m, t)$  and  $h(m, t)$ , the model predicts radial and transverse waveforms  $V_{pre}(t) = s(t) * v(m, t)$  and  $H_{pre}(t) = s(t) * h(m, t)$ . If  $m$  is a good model, then  $V_{pre}(t) \approx V(t)$  and  $H_{pre}(t) \approx H(t)$ , and thus  $v(m, t) * H(t) \approx h(m, t) * V(t)$ . We search for a model that minimizes the normalized difference  $E(m)$  between the two ‘cross convolution’ waveforms

$v(m, t) * H(t)$  and  $h(m, t) * V(t)$ . Figure 6 shows a graphical example of the cross-convolution method.

Since ML does not assume the fast and slow pulses are identically shaped, it can directly assess complex models without the need for apparent splitting parameters, and it does not require as complete a back-azimuth distribution (Menke and Levin, 2003). We also find it to be more robust in the presence of noise, which permits a more automated workflow than that of SplitLab: no waveform filtering is necessary, and small changes in the time window have little effect on the measurement.

We use the ML method to measure splitting for each seismogram assuming a single-layer model, and determine splitting at each station (Figure 4) by choosing the model that minimizes the total misfit across all events recorded by that station. We also tried two-layer models (discussed below), but with little success. For events with published splitting measurements (e.g., Yang et al., 2014), ML results are typically very similar to other methods.

Like the SC and RC methods, the ML method returns ‘null-split’ measurements when a seismogram is noisy, the polarization direction coincides with the fast or slow direction of anisotropy, or the single-layer model does not fit the observations well. In the ML results, null measurements tend to have large delay times and best-fitting models with fast directions parallel to the back azimuth. Null and noisy measurements do not need to be removed when calculating splitting parameters at a station, but we apply an additional automatic

quality control step to remove these questionable results from our plots of results for individual events. We discard all events with unphysically large delay times ( $>4$  s), then fit a smooth model to the remaining measurements and discard events more than 2.5 standard deviations from the smooth model. With nulls removed, the data set includes approximately 3100 measurements (Figure 3).



### III: RESULTS AND DISCUSSION

#### SKS Splits

Comparing seismograms across the region, we find that radial component SKS arrivals for the same events look similar at stations in NE and SE Oregon. Transverse SKS arrivals often differ between stations (as expected, if anisotropy varies across the region), but we find that most events produce well defined transverse SKS arrivals across the region. We do not see a systematic difference in noise characteristics between stations in NE and SE Oregon.

The fast axes of shear wave splitting measured at stations (Figure 4) tend to be oriented east-northeast. Fast axes beneath the Blue Mountains trend more northeast, and trend southeast in the western Snake River Plain. Delay times are quite variable, with maximum split times of  $\sim 2$  s in the High Lava Plains decreasing to an average of  $\sim 1$  s in northeast Oregon and nearby areas. Splitting measurements vary smoothly below stations, and we see no outliers among stations with  $>10$  measurements (stations with  $<10$  measurements are omitted from the figure for clarity).

In Figure 3 we back project the individual splitting events to their ray piercing points at a depth of 200 km (chosen visually to maximize the coherency of the plot). Because of the nonuniform distribution of global seismicity our data are dominated by events with back azimuths pointing to the west, and a large number of piercing points cluster to the west of the north-south oriented Wallowa2 array.

If complex SKS waveforms in NE Oregon were a result of near-field effects such as topographic signal-generated noise or crustal anisotropy, we would expect to see systematic differences in events with nearby piercing points measured at separate stations (with rays sampling the same mantle volume, but different regions of the crust). However, we do not see such a difference – results with nearby piercing points are consistent from station to station. Well constrained measurements with significantly different parameters overlap, but the variation in parameters does not appear to depend on station location.

We also produced a map of averaged splitting results (Figure 5). For each location, we stack the results shown in Figure 4 that are within 50 km of the location, with weighting a gaussian function of distance. In areas that are well covered by rays at 200 km depth, this map is overall similar to the station-averaged splitting map. Other than a poorly sampled region of northern Idaho, splitting time reaches a minimum of  $\sim 0.8$  s in the northeast corner of Oregon, where the average fast direction also rotates from east-northeast to north-northeast. Although this region of Oregon is not especially well sampled, the events shown there in Figure 3 include back azimuths facing both east and west, and the feature persists when averaging over larger bins.

We also tested for frequency dependence in the splitting results, which is associated with spatial variations in anisotropy. Splitting in both NE and SE Oregon varies somewhat depending on the frequency band, but we observe the highest degree of variability in NE Oregon. Although the effects of spatially

varying anisotropy are complex, higher frequencies are more sensitive at shallower depths (Saltzer et al., 2000). We note that if the seismograms are filtered at longer periods (i.e., 20-50 s), splitting is similar in NE and SE Oregon.

### Complex Anisotropy

As a simple way of assessing the evidence for complex anisotropy, we use the Menke and Levin (2003) misfit statistic  $E(\mathbf{m})$  between individual measurements of  $E(\mathbf{m})$  at each station. A vertically incident ray on a uniform anisotropic fabric with a horizontal fast axis produces identically shaped fast and slow pulses, and in the absence of noise the two cross-convolution waveforms match perfectly (e.g., Figure 6a and b). If the anisotropy is more complex, the fast and slow pulses are not generally identically shaped, and the cross-convolution waveforms do not match (e.g., Figure 6c and d).

For both the stacked station models (Figure 7a) and single event results (Figure 6b), we observe coherent patterns in the geographical distribution of misfit. Misfit is generally low on the periphery of the study region and increases toward NE Oregon. However, even though the average misfit increases in NE Oregon we observe many individual results with small misfit values. Although noisier records have greater misfit values, and individual events with greatest misfits tend to be noisy, records at stations in NE Oregon are not noisier than in the rest of the region. This suggests the poor misfit values in the NE Oregon

region indicate an anisotropy that is not well modeled by a single horizontal layer.

Considering the poor fit in NE Oregon, we also searched for two-layer models. Menke and Levin (2003) note that two-layer models are prone to overfitting because the four-parameter model (the fast axis orientation and delay time for each layer) is nonunique, and a two layer model with nearly parallel or perpendicular fast axis orientations is nearly equivalent to a single layer model. The ML method can theoretically identify two layers of anisotropy from a single record, but given that two-layer models are poorly constrained we stacked results from events with nearby piercing points. We apply an f-test to each two-layer result and retain only the models that improve the one-layer misfit statistic at a 95% confidence level.

Figure 8 shows the results of two-layer modeling. Where the two-layer models are successful, one of the layers is typically oriented close to the orientation of the best-fitting single layer model. The two-layer models often give a statistically significant improvement in the cross-convolution misfit, but misfit values are still much larger in NE Oregon. In many cases the best-fitting fast axes are near perpendicular and one layer is parallel to the single-layer model, suggesting that the variance reduction is due to overfitting of noise. The consistency of the results suggests that anisotropy varies with depth, but a two-layer model does not appear to be enough to describe anisotropy in northeast Oregon. However, we note that the most densely sampled area of the High Lava

Plains produces successful two-layer models that do not fall in the “nearly one layer” regime, consistent with Wagner & Long’s (2013) observations of strong vertical heterogeneity.

### Finite Frequency Modeling

Given that our results in NE Oregon are frequency dependent (implying spatially varying anisotropy) and that the two-layer anisotropy model performs poorly, we hypothesize that upper mantle anisotropy is laterally heterogeneous. If the Wallowa anomaly represents delaminated Farallon oceanic lithosphere (e.g., Darold & Humphreys, 2013), we may expect 'fossil' anisotropy aligned with the spreading direction at the site of lithosphere formation (albeit possibly modified by the delamination event), and not necessarily with present flow-induced anisotropy elsewhere in the upper mantle (Audet, 2013). Flow due to the Wallowa anomaly detachment would also have created an anisotropic fabric in the upper mantle, though that fabric may have been overprinted by more recent deformation.

We use a forward model to investigate the effects of laterally heterogeneous anisotropy. We use the three-dimensional finite-frequency sensitivity kernels of Favier and Chevrot (2003) to predict splitting intensity from a hypothesized anisotropic structure, and predict station-averaged splitting by fitting a sine function to splitting intensity as a function of back azimuth, as described by Chevrot (2000). Although the splitting as measured by splitting

intensity is not necessarily the same as that measured by cross-convolution, we expect that results for the two methods are similar (Romanowicz & Yuan, 2012). We incorporate the effects of the nonuniform back azimuth distribution by performing the calculation at randomly selected back azimuths from the list of events.

The Favier & Chevrot (2003) sensitivity kernels imply that a vertically incident shear wave at 0.1 Hz (typical for teleseismic SKS phases) at a depth of 200 km is sensitive to a mantle volume with a radius of approximately 150 km, and the peak sensitivity occurs approximately 60 km from the ray path. The observed delay time is more sensitive to spatial variations in anisotropy than the observed fast polarization direction. In eastern Oregon, we observe significant differences in anisotropy over distances comparable to the size of the sensitivity kernel. Because the radius of the Wallowa anomaly in map view is approximately 40 km, it is plausible that anisotropy in the anomaly itself does not have a distinct signal at the frequencies we use. However, heterogeneity at this scale could explain our erratic splitting measurements in northeast Oregon.

We use a model of an anisotropic inclusion with similar geometry to the Wallowa anomaly to test our interpretations of the finite frequency kernels. The model consists of a cylindrical volume with a radius of 40 km extending from a depth of 100 to 300 km, inset in an 'asthenospheric' layer extending from 150 to 300 km. Both the Wallowa anomaly and asthenospheric layer have a uniform 5% anisotropy (corresponding to a delay time of 1.5 seconds in the asthenosphere).

The fast axis is oriented N80°E in the asthenospheric layer and N30°E in the anomaly. Shear wave velocity is 4.9 km/s. Ray theory predicts a splitting time of approximately 1.5 seconds away from the Wallowa anomaly and 2 seconds at stations above the anomaly.

Predicted SKS splitting (Figure 9) exhibits little variation in fast axis orientation, but the delay time varies substantially over an area roughly the size of the finite frequency kernel. Opposite the ray theoretical predictions, observed splitting times decrease at stations above the anomaly. The decrease in splitting time extends over an area with a radius of roughly 100 km, significantly larger than the anomaly itself. If the Wallowa anomaly is isotropic, or if anisotropy in the anomaly is highly variable on small scales, it causes an average decrease in splitting time from ~1.5 to ~1.2 s (Figure 9b). A larger decrease in splitting time requires the anomaly to be anisotropic, but oriented nearly perpendicular to the asthenospheric flow direction.

#### IV: CONCLUSIONS

We use a largely automated method to compile approximately 3100 non-null shear-wave splitting measurements in the northwest United States. Our measurements are generally consistent with previous studies using different methodologies, but our study has much improved resolution.

Shear-wave splitting in the northwest United States appears to be roughly consistent with a simple model of anisotropy, with fast directions trending east-to-northeast. We attribute this to simple shear flow driven by motion of the North American plate, with the systematic deviations attributable to flow modification by the Cascadia subduction zone or Pacific plate motion. We observe particularly large delay times, and characteristics of simple anisotropy, in the High Lava Plains and Snake River Plain regions. Observed fast directions suggest east-west oriented flow beneath the High Lava Plains that is redirected toward the northeast by a low viscosity region associated with low seismic velocities beneath the western Snake River Plain.

The shear-wave splitting signal in the area of northeast Oregon expresses an anisotropy that is inconsistent with layered models. My modeling of multi-layered structures and structures with lateral variations suggests that the anisotropic structure beneath northeast Oregon has relatively strong lateral heterogeneity. This region corresponds with the seismically imaged “Wallowa” high-velocity anomaly under northeast Oregon. Models imply that anisotropy in the Wallowa anomaly can produce a region of reduced split times (and



presumably more complex waveforms) several times larger in map view than the anomaly itself, and approximately the same size as the area in which observed seismic waveforms are most complicated.

## APPENDIX: FIGURES

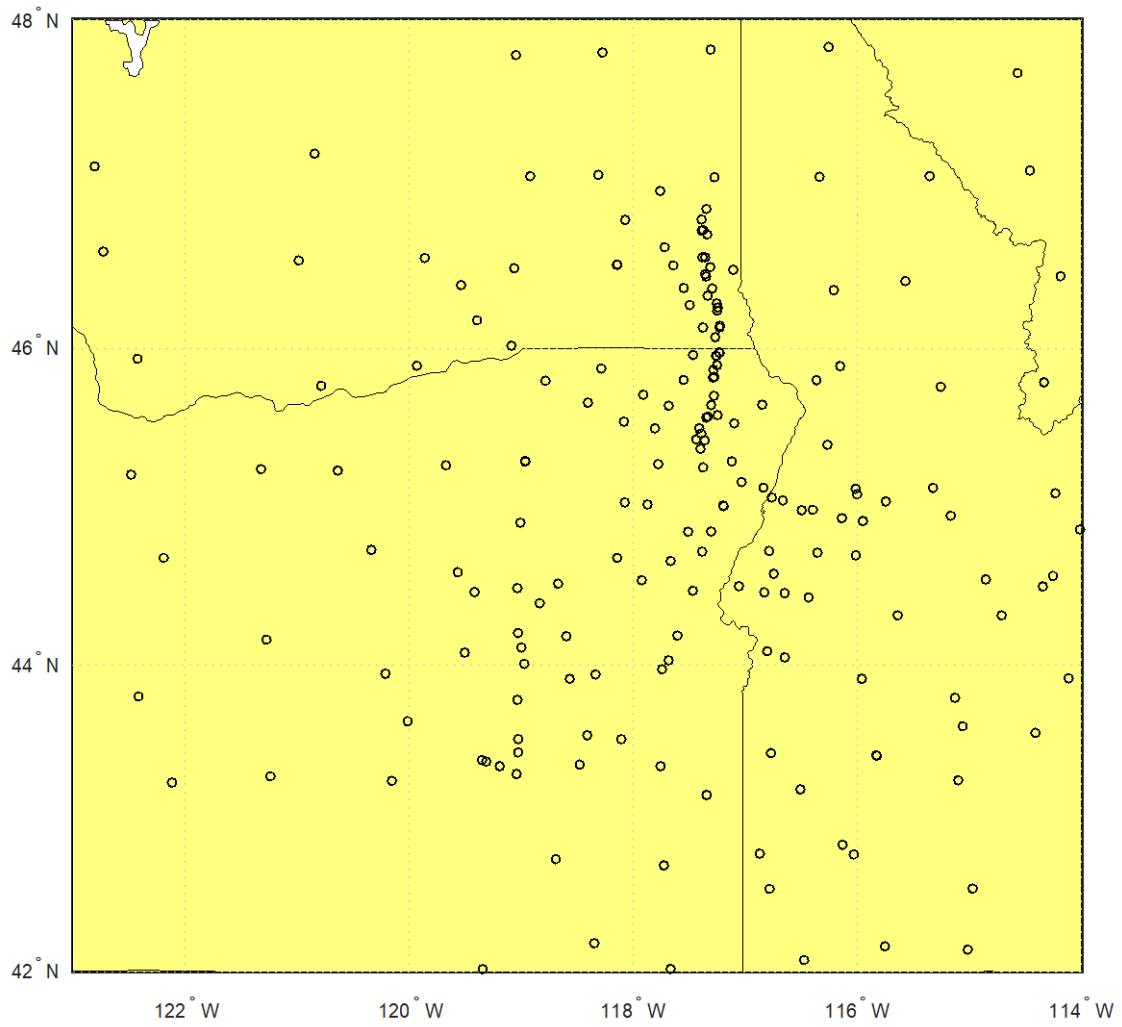


*Figure 1: Location of the broadband seismic stations used in my study.*

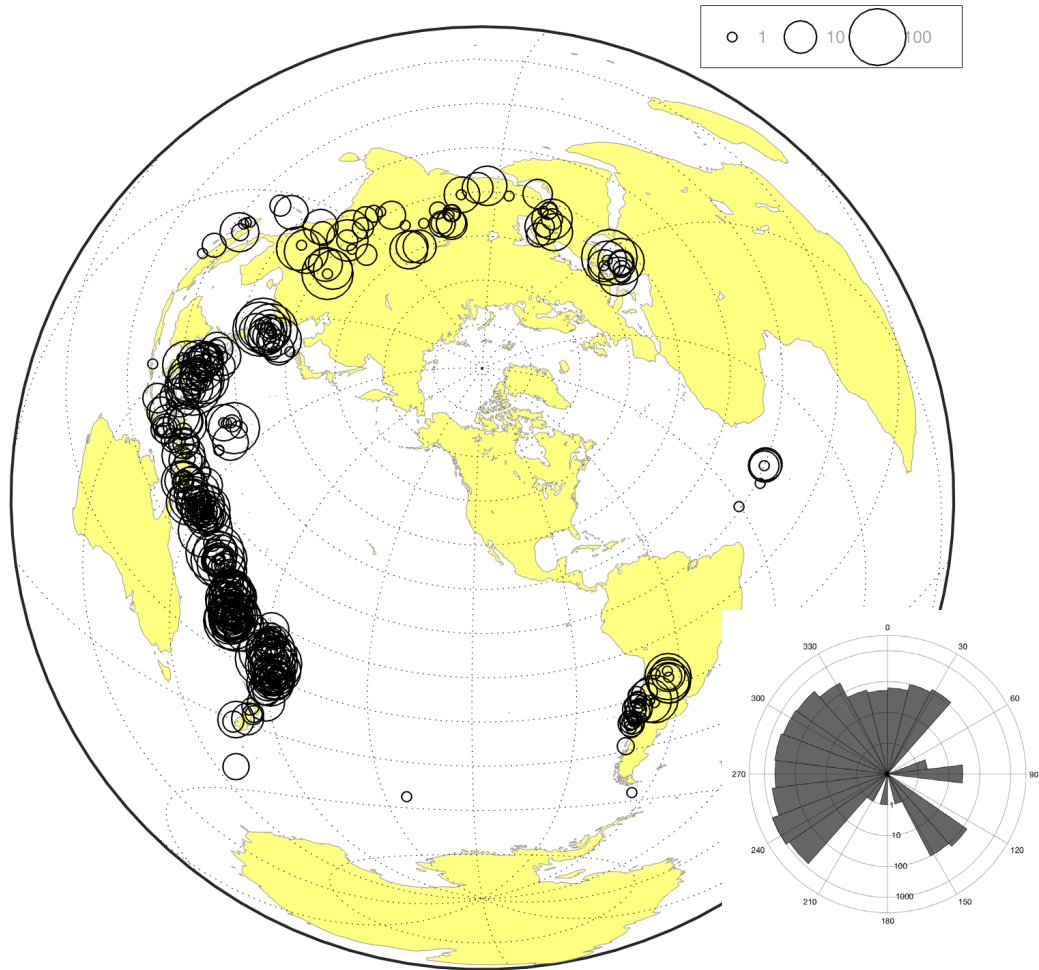


*Figure 2: Distribution of earthquakes and number of seismograms per earthquake. Inset: Distribution of backazimuths for all seismograms (note logarithmic scale).*

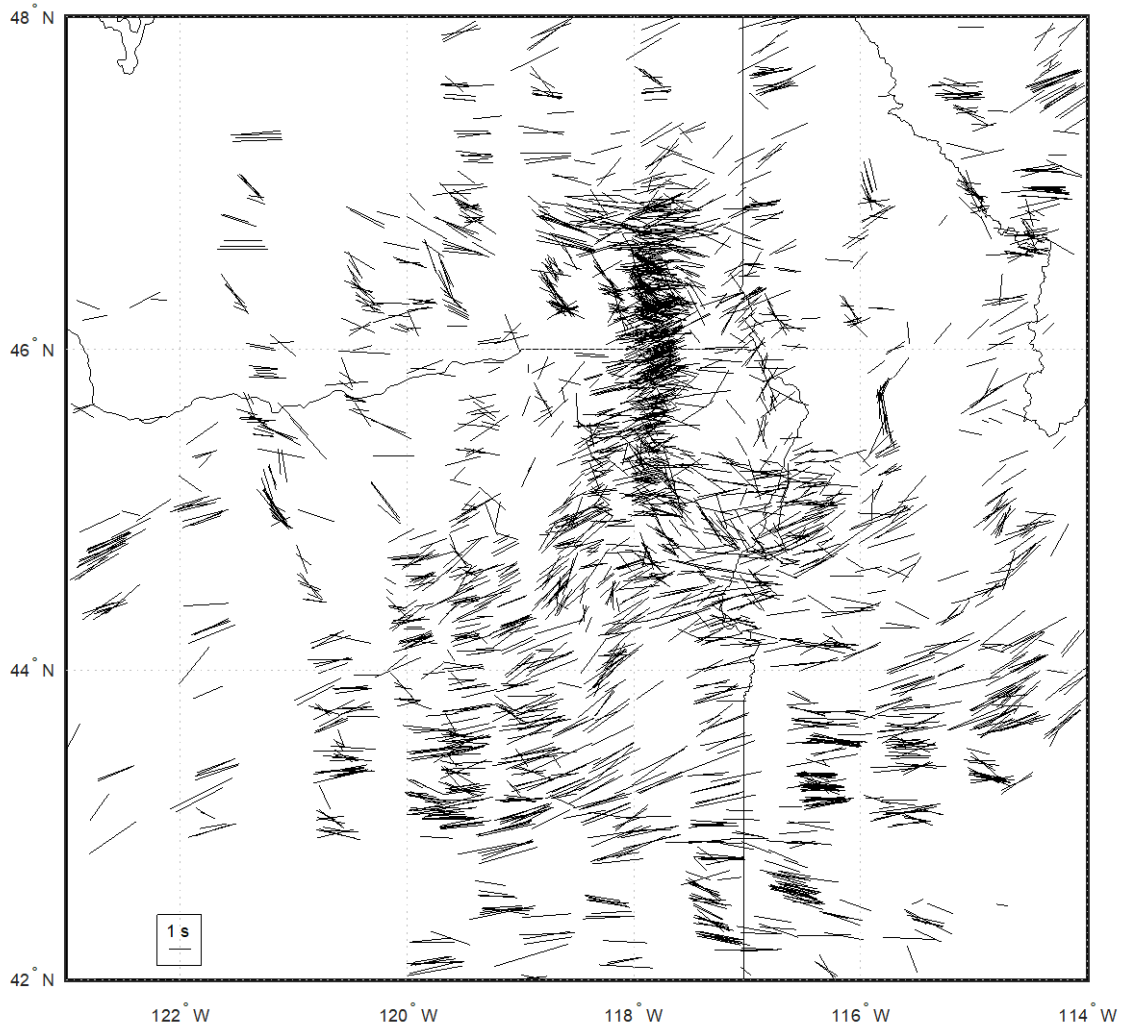


*Figure 3: Non-null splitting results, plotted at the piercing points of the rays at 200 km.*

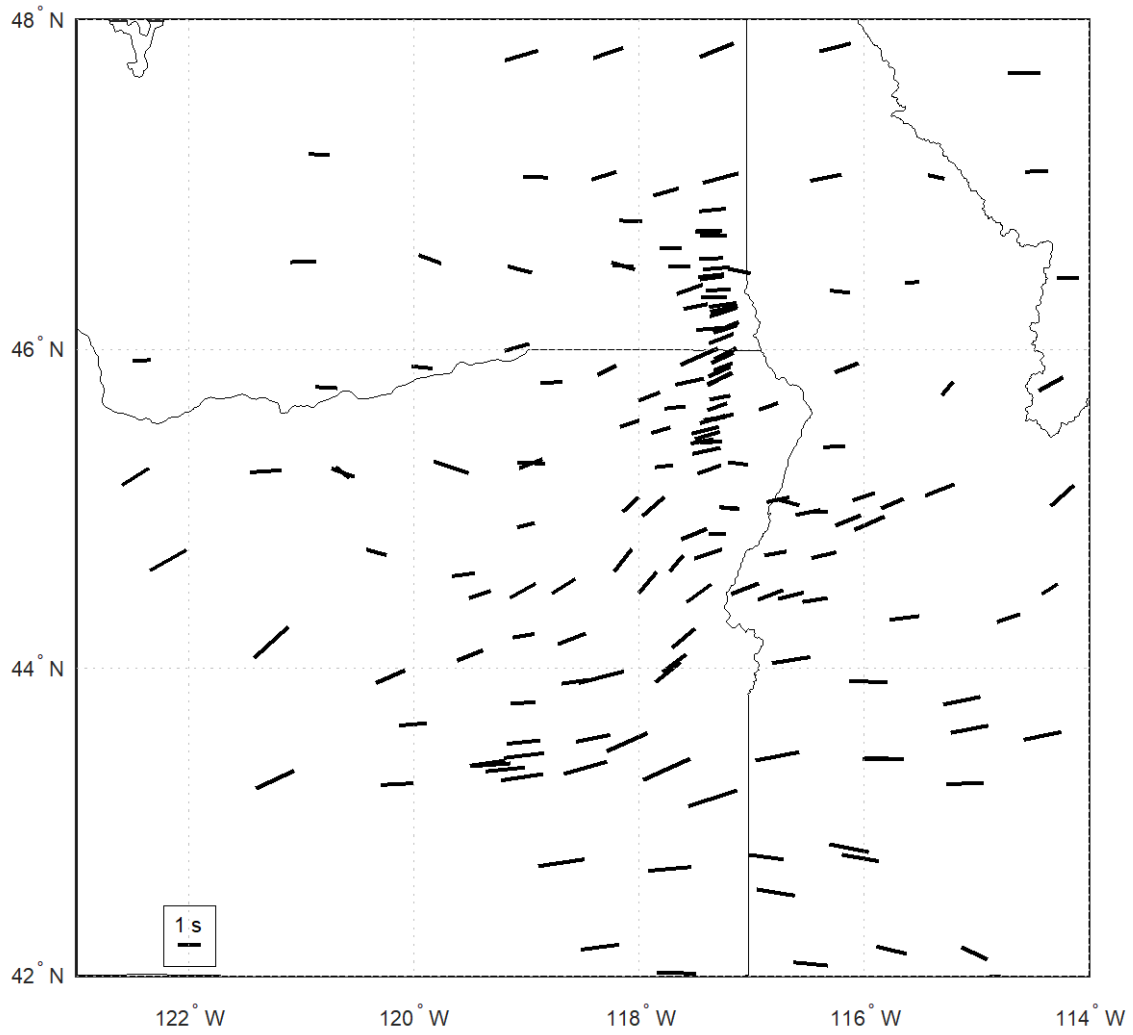
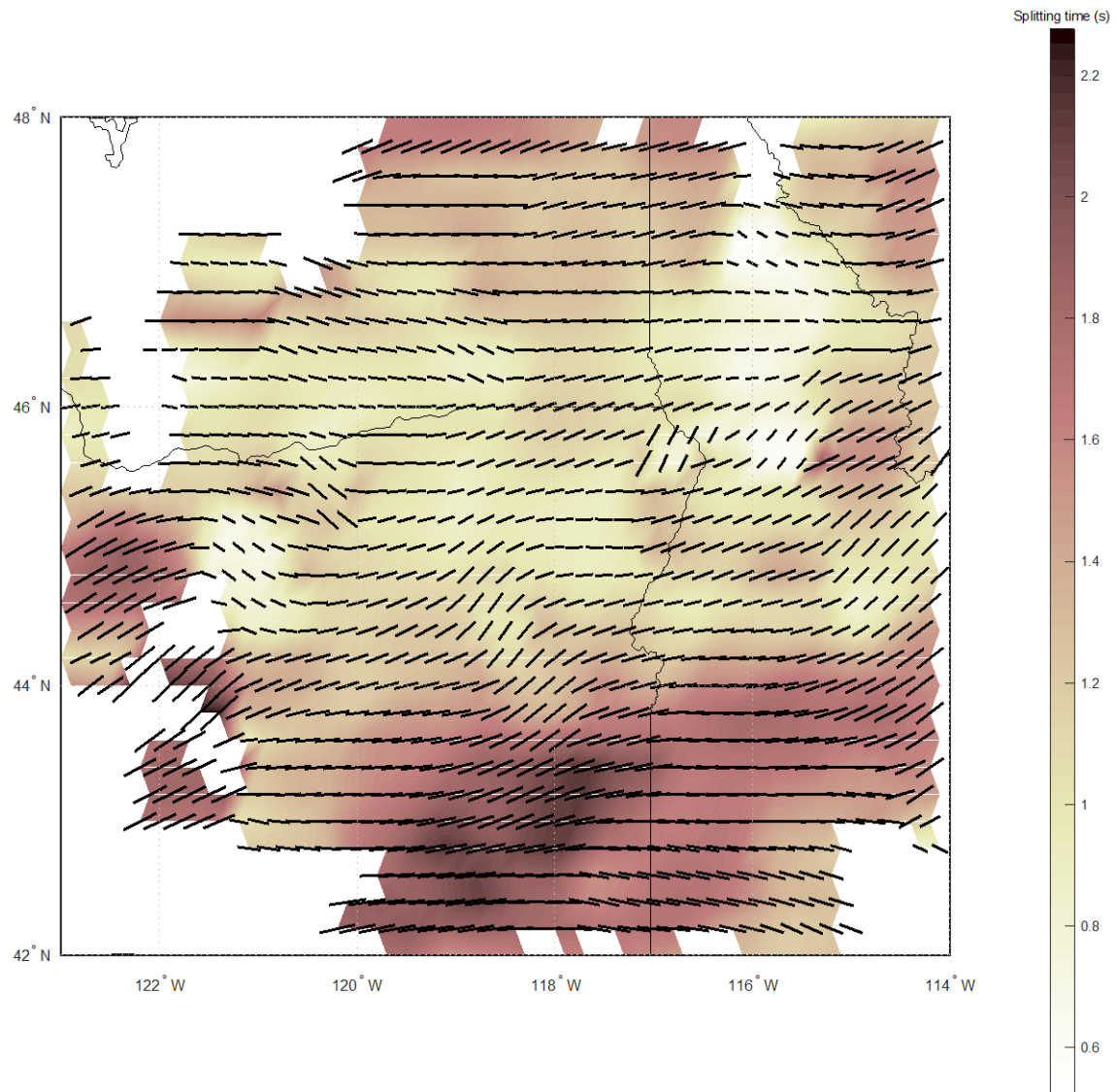


Figure 4: Average splitting estimates for stations with  $\geq 10$  events recorded.



*Figure 5: Average one-layer splitting estimates, produced by stacking measurements at their piercing points in overlapping circular bins with radius 50 km.*

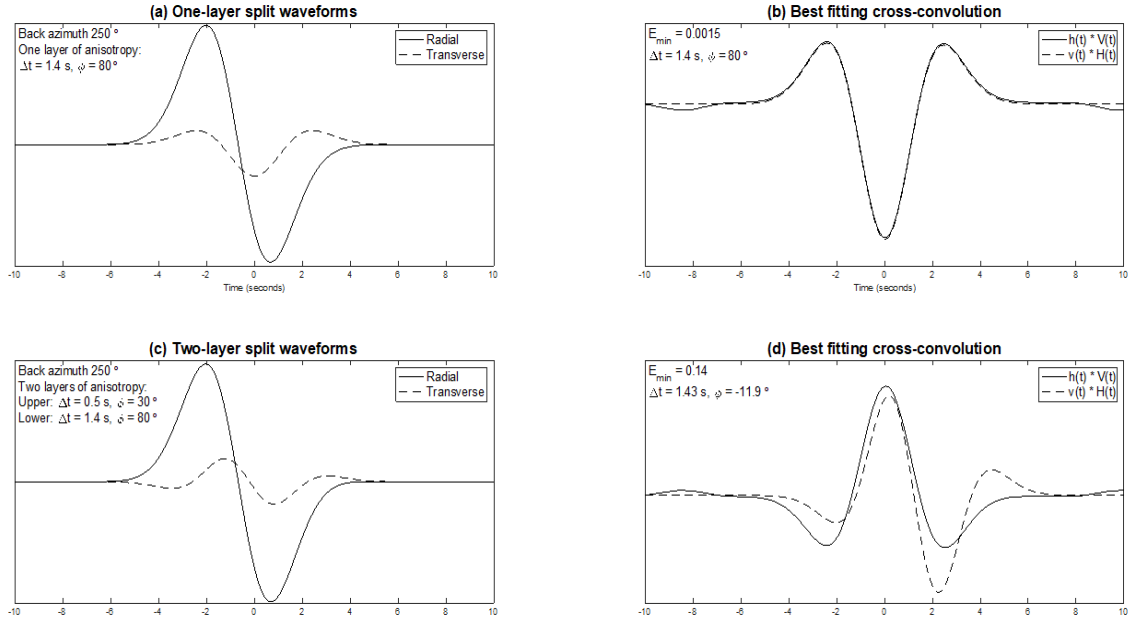


Figure 6: Synthetic example of the cross-convolution method. (a) Predicted radial and transverse waveforms due to one-layer anisotropy model. (b) Cross-convolution waveforms, predicted splitting parameters  $\Delta t$  and  $\phi$  and misfit statistic  $E$  for a one-layer model applied to (a). (c) Predicted radial and transverse waveforms due to two-layer anisotropy model. (d) Cross-convolution waveforms, predicted splitting parameters and misfit statistic for a one-layer model applied to (c).

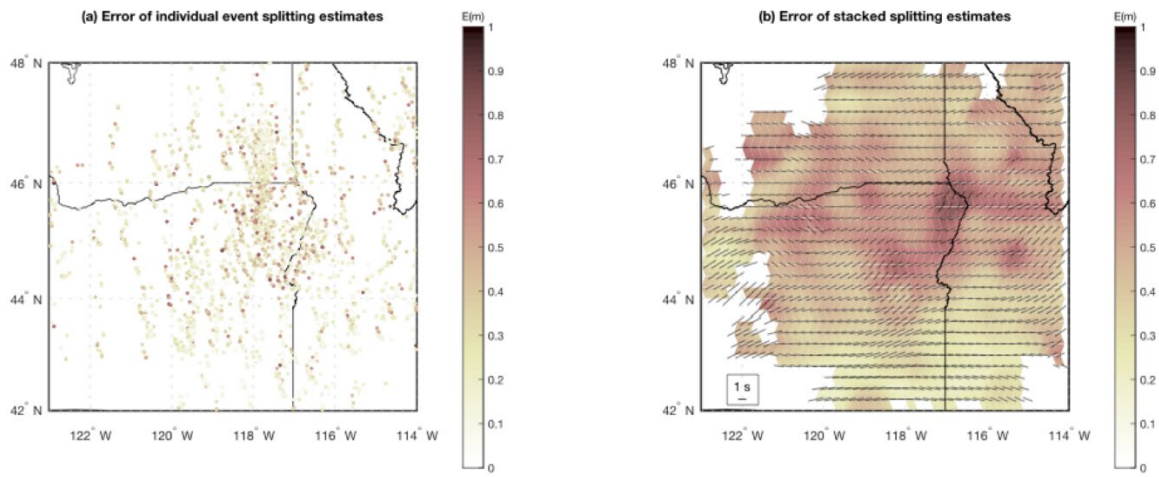
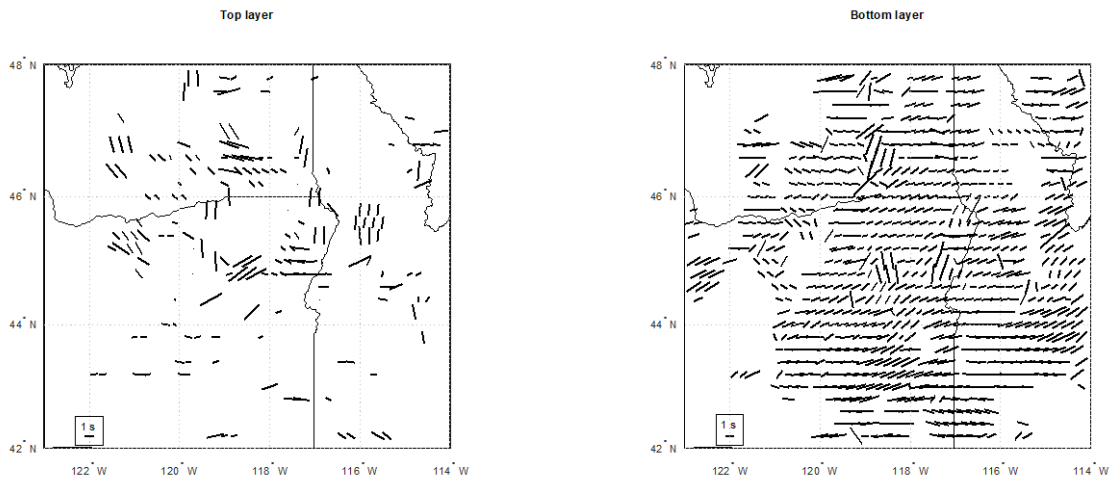


Figure 7: Cross-convolution measurement misfit,  $E(m)$ . (a) Misfit of the best-fitting one-layer models for each event, plotted on the ray piercing points at 200 km. (b) Misfit of the stacked splitting estimates from Figure 5.





*Figure 8: Best fitting two-layer anisotropic models. Only two-layer models with a statistically significant (at the 95% level) improvement over the one-layer model are shown – if the improvement is not significant, the one-layer model is shown instead. Events with nearby piercing points are stacked as in Figure 5.*

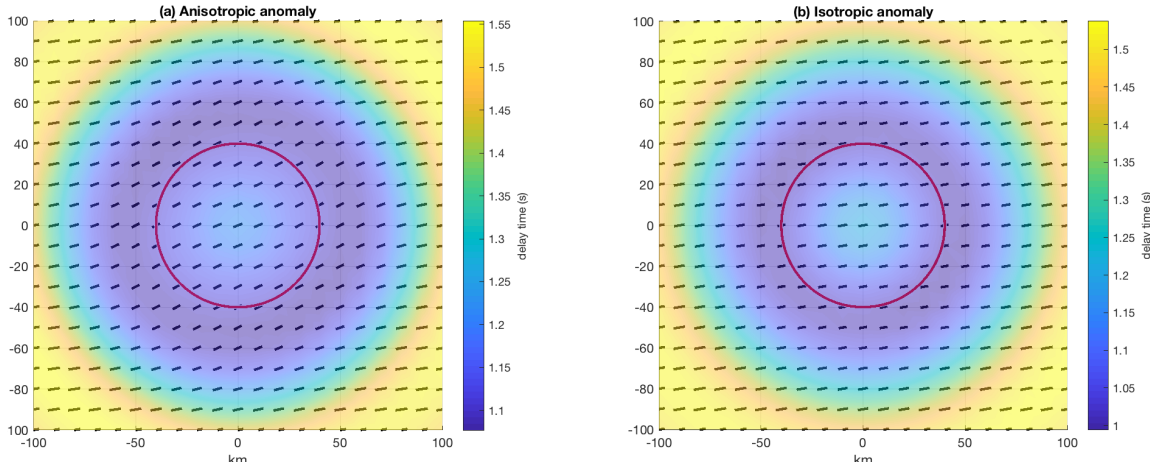


Figure 9: Finite-frequency synthetic model of splitting above a structure analogous to the Wallowa anomaly (described in text), modeled with (a) and without (b) anisotropy in the anomaly. Circles indicate the boundaries of the anomalous structure.

## REFERENCES CITED

- Audet, P. (2013). Seismic anisotropy of subducting oceanic uppermost mantle from fossil spreading. *Geophysical Research Letters*, *40*, 173-177.
- Becker, T. W., Schulte-Pelkum, V., Blackman, D. K., Kellogg, J. B., & O'Connell, R. J. (2006). Mantle flow under the western United States from shear-wave splitting. *Earth and Planetary Science Letters*, *237*(3-4), 235-251.
- Bowman, J. R., & Ando, M. (1987). Shear-wave splitting in the upper-mantle wedge above the Tonga subduction zone. *Geophysical Journal International*, *88*(1), 25-41.
- Castellanos, J. C., Perry-Houts, J., Clayton, R. W., & Humphreys, E. (2019a). Crustal anisotropy as a window to mantle dynamics: A case study on the western United States. Abstract presented at 2019 AGU Fall Meeting, San Francisco.
- Castellanos, J. C., Perry-Houts, J., Clayton, R. W., Kim, Y., Stanciu, A. C., Niday, B., & Humphreys, E. (2019b). Seismic anisotropy reveals crustal flow driven by mantle vertical loading in the Pacific NW. Manuscript submitted for publication.
- Chevrot, S. (2000). Multichannel analysis of shear-wave splitting. *Journal of Geophysical Research: Solid Earth*, *105*(B9), 21579-21590.
- Crotwell, H. P., Owens, T. J., & Ritsema, J. (1999). The TauP Toolkit: Flexible seismic travel-time and ray-path utilities. *Seismological Research Letters*, *70*(2), 154-160.
- Darold, A., & Humphreys, E. (2013). Upper mantle seismic structure beneath the Pacific Northwest: A plume-triggered delamination origin for the Columbia River flood basalt eruptions. *Earth and Planetary Science Letters*, *365*, 232-242.
- Druken, K. A., Long, M. D., & Kincaid, C. (2011). Patterns in seismic anisotropy driven by rollback subduction beneath the High Lava Plains. *Geophysical Research Letters*, *38*(13).
- Favier, N., & Chevrot, S. (2003). Sensitivity kernels for shear wave splitting in transverse isotropic media. *Geophysical Journal International*, *153*(1), 213-228.

- Lin, F.-C., Ritzwoller, M. H., Yang, Y., Moschetti, M. P., & Fouch, M. J. (2011). Complex and variable crustal and uppermost mantle seismic anisotropy in the western United States. *Nature Geoscience*, 4(1), 55.
- Liu, L., & Stegman, D. R. (2011). Segmentation of the Farallon slab. *Earth and Planetary Science Letters*, 311(1-2), 1-10.
- Long, M. D., Gao, H., Klaus, A., Wagner, L. S., Fouch, M. J., James, D. E., & Humphreys, E. (2009). Shear wave splitting and the pattern of mantle flow beneath eastern Oregon. *Earth and Planetary Science Letters*, 288(3-4), 359-369.
- Lowry, A. R., Ribe, N. M., & Smith, R. B. (2000). Dynamic elevation of the Cordillera, western United States. *Journal of Geophysical Research: Solid Earth*, 105(B10), 23371-23390.
- McCaffrey, R., King, R. W., Payne, S. J., & Lancaster, M. (2013). Active tectonics of northwestern U.S. inferred from GPS-derived surface velocities. *J. Geophys. Res. Solid Earth*, 118(2), 709-723.
- Menke, W., & Levin, V. (2003). The cross-convolution method for interpreting SKS splitting observations, with application to one and two-layer anisotropic earth models. *Geophysical Journal International*, 154(2), 379-392.
- Romanowicz, B., & Yuan, H. (2012). On the interpretation of SKS splitting measurements in the presence of several layers of anisotropy. *Geophysical Journal International*, 188(3), 1129-1140.
- Saltzer, R. L., Gaherty, J. B., & Jordan, T. H. (2000). How are vertical shear-wave splitting measurements affected by variations in the orientation of azimuthal anisotropy with depth? *Geophysical Journal International*, 141(2), 374-390.
- Schmandt, B., & Humphreys, E. (2010). Complex subduction and small-scale convection revealed by body-wave tomography of the western United States upper mantle. *Earth and Planetary Science Letters*, 297(3-4), 435-445.
- Silver, P. G., & Chan, W. W. (1991). Shear wave splitting and subcontinental mantle deformation. *Journal of Geophysical Research: Solid Earth*, 96(B10), 16429-16454.
- Silver, P. G., & Savage, M. K. (1994). The interpretation of shear-wave splitting parameters in the presence of two anisotropic layers. *Geophysical Journal International*, 119(3), 949-963.

- Wüstefeld, A., Bokelmann, G., Zaroli, C., & Barruol, G. (2008). SplitLab: A shear-wave splitting environment in Matlab. *Computers & Geosciences*, 34(5), 515-528.
- Wagner, L. S., & Long, M. D. (2013). Distinctive upper mantle anisotropy beneath the High Lava Plains and Eastern Snake River Plain, Pacific Northwest, USA. *Geochemistry, Geophysics, Geosystems*, 14(10), 4647-4666.
- Wang, W., & Becker, T. W. (2019). Upper mantle seismic anisotropy as a constraint for mantle flow and continental dynamics of the North American plate. *Earth and Planetary Science Letters*, 514, 143-155.
- Yang, B. B., Liu, K. H., Dahm, H. H., & Gao, S. S. (2016). A uniform database of teleseismic shear-wave splitting measurements for the western and central United States: December 2014 update. *Seismological Research Letters*, 87(2A), 295-300.
- Zhou, Q., Hu, J., Liu, L., Chaparro, T., Stegman, D. R., & Faccenda, M. (2018). Western US seismic anisotropy revealing complex mantle dynamics. *Earth and Planetary Science Letters*, 500, 156-167.